GEOLOGY | THE GEOLOGICAL SOCIETY OF AMERICA®

https://doi.org/10.1130/G46916.1

Manuscript received 26 August 2019
Revised manuscript received 23 November 2019
Manuscript accepted 26 November 2019

A significant acceleration of ice volume discharge preceded a major retreat of a West Antarctic paleo–ice stream

Philip J. Bart[1] and Slawek Tulaczyk[2]
[1]Department of Geology and Geophysics, Louisiana State University, Baton Rouge, Louisiana 70803, USA
[2]Department of Earth and Planetary Sciences, University of California Santa Cruz, Santa Cruz, California 95064, USA

ABSTRACT

For the period between 14.7 and 11.5 cal. (calibrated) kyr B.P, the sediment flux of Bindschadler Ice Stream (BIS; West Antarctica) averaged 1.7×10^8 m^3 a^{-1}. This implies that BIS velocity averaged 500 ± 120 m a^{-1}. At a finer resolution, the data suggest two stages of ice stream flow. During the first 2400 ± 400 years of a grounding-zone stillstand, ice stream flow averaged 200 ± 90 m a^{-1}. Following ice-shelf breakup at 12.3 ± 0.2 cal. kyr B.P., flow accelerated to 1350 ± 580 m a^{-1}. The estimated ice volume discharge after breakup exceeds the balance velocity by a factor of two and implies ice mass imbalance of –40 Gt a^{-1} just before the grounding zone retreated >200 km. We interpret that the paleo-BIS maintained sustainable discharge throughout the grounding-zone stillstand first due to the buttressing effect of its fringing ice shelf and then later (i.e., after ice-shelf breakup) due to the stabilizing effects of grounding-zone wedge aggradation. Major paleo–ice stream retreat, shortly after the ice-shelf breakup that triggered the inferred ice flow acceleration, substantiates the current concerns about rapid, near-future retreat of major glaciers in the Amundsen Sea sector where Pine Island and Thwaites Glaciers are already experiencing ice-shelf instability and grounding-zone retreat that have triggered upstream-propagating thinning and ice acceleration.

INTRODUCTION

Analyses of modern ice stream systems have provided much information about their behavior (Alley et al., 1986; Rignot et al., 2004; Vieli et al., 2007; Scambos et al., 2009). These studies have shown that ice streams accelerate when buttressing is reduced by either ice shelf thinning and/or collapse. The flow acceleration is of concern because models suggest that it may trigger a tipping-point response in which the extent of grounded ice abruptly contracts (Alley et al., 2015; Pattyn, 2018). On the other hand, sediment transport by ice streams may also result in rapid sedimentation at the grounding zone. Subglacial and grounding-zone sedimentation aggradation may act as a negative feedback that counters dynamic thinning of the ice stream and stabilizes the ice-stream grounding zones (e.g., Alley et al., 2007).

The understanding of modern ice-stream sediment flux (e.g., Alley et al., 1986) has been highly instrumental in interpreting the glacial landforms and deposits on the outer continental shelves that formed after the Last Glacial Maximum (LGM) (Anderson, 1999; Ó Cofaigh et al., 2002; Jakobsson et al., 2012; Klages et al. 2014; Prothro et al., 2018). Detailed analyses of the now ice-free areas, where grounding-zone wedges (GZWs) are exposed on the seafloor, provide records of the dynamic retreat history of marine-based ice streams. These retreat records are important because they provide insight into the processes and rates needed to predict future ice retreat in West Antarctica (e.g., Bingham et al., 2017).

Here we use published data from the Whales Deep Basin (eastern Ross Sea) to quantify the evolution of ice and sediment fluxes that preceded a >200 km retreat of the paleo–Bindschadler Ice Stream (paleo-BIS; West Antarctica) from the outer continental shelf. The Whales Deep Basin contains a large-volume overlapping stack of GZWs, which have been mapped with seismic and subbottom profiles and multibeam bathymetric data (Bart et al., 2017a, 2017b) and individually cored (McGlannan et al., 2017) (Figs. 1A–1C). This stratigraphic framework is constrained by radiocarbon ages (Bart et al., 2018) and provides evidence indicating that rapid GZW construction delayed the retreat of grounded ice for hundreds of years after the breakup of its fringing ice shelf.

SEDIMENT AND ICE DISCHARGE FROM THE PALEO–BINDSCHADLER ICE STREAM

Radiocarbon ages from benthic foraminifera (Bart et al., 2018) (Table 1) indicate that the paleo-BIS grounding line had retreated 70 km from its maximum (LGM) position by 14.7 ± 0.4 cal. (calibrated) kyr B.P. and stabilized at the Whales Deep Basin GZW with a fringing ice shelf in front of it. Shortly after 12.3 ± 0.6 cal. kyr B.P., this ice shelf collapsed, but the grounding line maintained its position until 11.5 ± 0.3 cal. kyr B.P. Hence, grounding-line stillstand at the Whales Deep Basin GZW lasted for 3.2 ± 0.7 k.y., with the ice-shelf breakup dividing it into two distinct phases.

The constraints on the GZW sediment volume and its depositional time frame (Bart et al., 2017a, 2017b, 2018; McGlannan et al., 2017) provide an opportunity to reconstruct ice discharge history from the paleo-BIS at the time of GZW deposition (Table 1). We define the average sediment flux rate, q, as the ratio of the total volume of deposited sediments, V, and the duration of deposition, ΔT. We express the sediment flux rate across the grounding line as a product of the ice stream width, W, the effective sediment thickness, h, as well as the average sediment transport velocity, u_s, which itself is expressed as a fraction, f, of the ice stream flow velocity, U:

$$q \equiv \frac{V}{\Delta T} = u_s Wh = fUWh. \quad (1)$$

Here we assume that till-bedded ice streams have constant velocity throughout ice thickness and width (e.g., Tulaczyk et al., 2000). For basal debris transport in ice, f is equal to 1 because sediments travel with the same velocity as ice itself, and we take h to be the equivalent thickness of a till layer that would form if sediments in the debris-laden basal ice would form a till layer with porosity of 40% (e.g., 3.5 ± 0.6 m

CITATION: Bart, P.J., and Tulaczyk, S., 2020, A significant acceleration of ice volume discharge preceded a major retreat of a West Antarctic paleo–ice stream: Geology, v. 48, p. , https://doi.org/10.1130/G46916.1

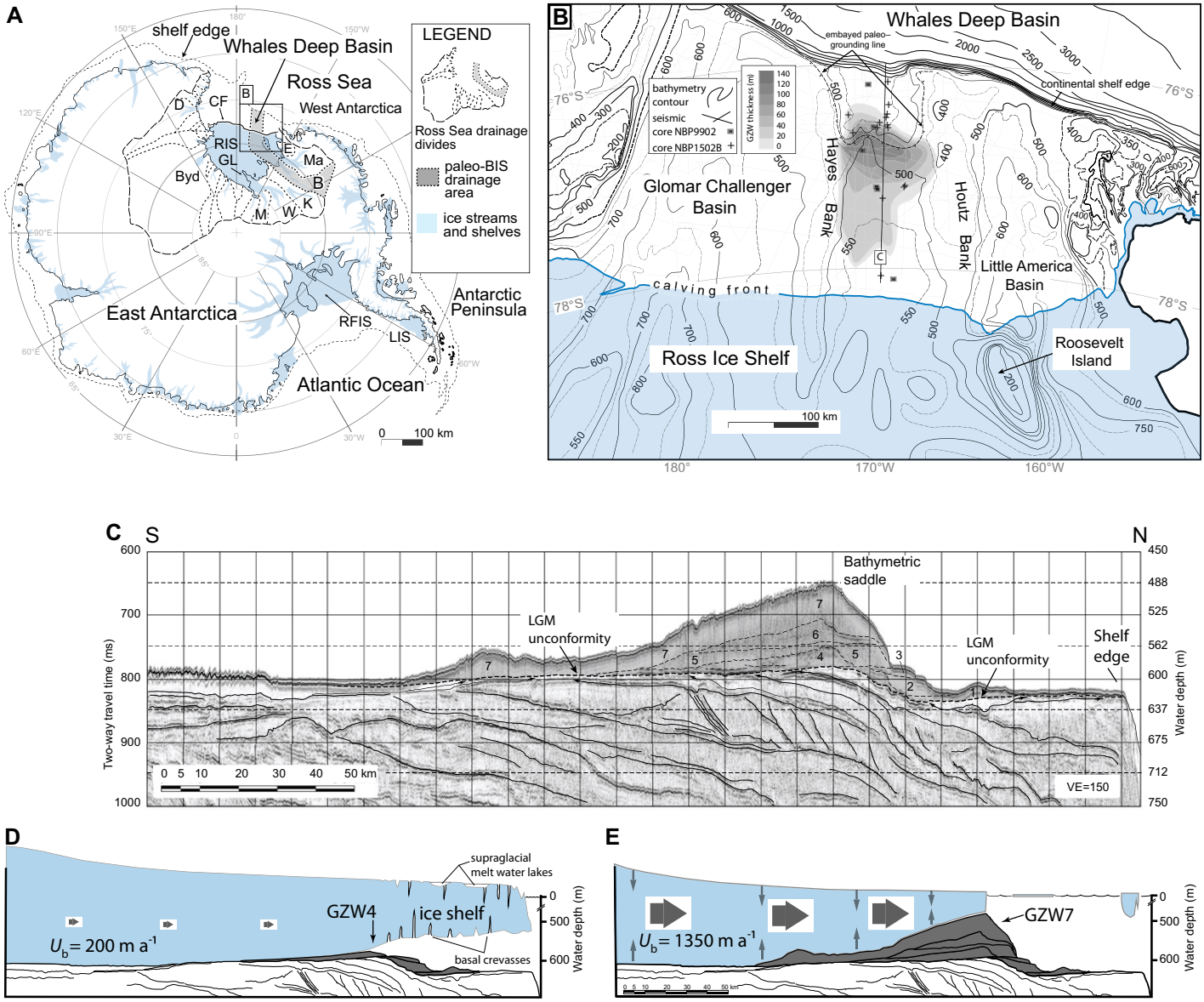

Figure 1. (A) Map of Antarctica showing ice streams and buttressing ice shelves. Dashed lines in continental interiors demarcate drainage areas of the East and West Antarctic Ice Sheets that converge into the Ross Sea. Gray shading shows the paleo–Bindschadler Ice Stream (paleo-BIS) drainage area during the Last Glacial Maximum (LGM). B—Bindschadler Ice Stream; D—David Glacier; Byd—Byrd Glacier; M—Mercer Ice Stream; W—Whillans Ice Stream; K—Kamb Ice Stream; Ma—MacAyeal Ice Stream; E—Echelmeyer Ice Stream; CF—calving front; RIS—Ross Ice Shelf; GL—grounding line; RFIS—Ronne-Filchner Ice Shelf; LIS—Larsen Ice Shelf. Modern-day shelf edge position is shown as short-dash line. (B) Bathymetry of the eastern Ross Sea continental shelf, from Davey and Nitsche (2005). Paleo-BIS was confined to Whales Deep Basin between the Hayes and Houtz Banks. Light-gray rectilinear lines are locations of seismic data. Gray squares are cores acquired by Mosola and Anderson (2006), and crosses are those described by McGlannan et al. (2017). NBP9902 and NBP1502B refer to R/V *Nathaniel B. Palmer* cruises. Gray shading shows thickness of grounding-zone wedges (GZWs) mapped from the seismic data by Bart et al. (2017b) (C; 1–7 are GZWs, VE—vertical exaggeration). (D) Interpretation of paleo-BIS during deposition of GZW4 prior to ice-shelf breakup. U_b is the balance ice velocity at the grounding line prior to ice-shelf breakup. (E) Interpretation of paleo-BIS during deposition of GZW7 prior to ice-shelf breakup.

TABLE 1. ESTIMATES OF SEDIMENT FLUX, YIELD, AND VELOCITY OF THE PALEO-BINDSCHADLER ICE STREAM, WEST ANTARCTICA

Whales Deep Basin grounding	Grounding-zone wedge volume (×10^{11} m^3)	Grounding chronologies (cal. kyr B.P.)			Grounding duration (yr)	Paleo-BIS sediment flux (10^8 m^3 a^{-1})	Paleo- BIS drainage area (×10^{11} m^2)	Estimated sediment yield (mm a^{-1})	Estimated paleo-BIS velocity (m a^{-1})
		Onset of OCS grounding	Paleo–ice-shelf breakup	End of OCS grounding					
Total	5.34	14.7 ± 0.4	12.3 ± 0.2	11.5 ± 0.3	3200 ± 700	1.7 ± 0.77	2.33	0.7 ± 0.21	500 ± 120
Pre-ISBU	1.60	14.7 ± 0.4	12.3 ± 0.2	—	2400 ± 400	0.67 ± 0.2	2.33	0.3 ± 0.1	200 ± 90
Post-ISBU	3.74	—	12.3 ± 0.2	11.5 ± 0.3	800 ± 300	4.7 ± 1.0	2.33	2.0 ± 0.4	1350 ± 580

Note: OCS—outer continental shelf; BIS—Bindschadler Ice Stream; ISBU—ice-shelf breakup. "Total" refers to deposits of grounding-zone wedges (GZWs) GZW1 through GZW7. Post-glacial sediment drape is not included in the quantification of GZW volume (see the Data Repository [see text footnote 1]). "Pre-ISBU" refers to deposits of GZW1 through GZW4. "Post-ISBU" refers to deposits of GZW5 through GZW7.

of till from the observed 2.1 ± 0.4 m of pure debris reported by Christoffersen et al. [2010] in the basal ice of Kamb Ice Stream, which is adjacent to BIS). For subglacial till transport, f may vary in space and time (e.g., Alley et al. [1987] versus Engelhardt and Kamb [1998]), and h is the thickness of the actively deforming till layer, which appears to be on decimeter scale (Engelhardt and Kamb, 1998; Hodson et al., 2016). Such small h is consistent with the contention of Christoffersen et al. (2010) that sediment advection in basal ice is the primary mode of sediment transport in West Antarctic ice streams. Thick and debris-rich basal ice has been found in a borehole drilled in Whillans Ice Stream (Tulaczyk et al., 2014).

Equation 1 can be rearranged to solve for the average ice velocity across the grounding line as a function of sediment flux:

$$U = q/(fWh). \quad (2)$$

Using the sediment flux values from Table 1, ice stream width of $W = 100$ km (the average width of the trough at the 500 m contour of the paleo-BIS presented by Danielson and Bart [2019]), and values of f and h based on Christoffersen et al. (2010) ($f = 1$, $h = 3.5 \pm 0.6$ m; see the GSA Data Repository[1] for a discussion of uncertainties), we estimate the average ice velocity for the entire period of GZW deposition to be 500 ± 120 m a^{-1}, whereas for the period preceding and after ice-shelf breakup at 12.3 ± 0.6 cal. kyr B.P., the ice stream velocity is estimated to have averaged 200 ± 90 m a^{-1} and 1350 ± 580 m a^{-1}, respectively (Fig. 2B). The first two values are consistent with the range of modern ice stream velocities in this part of West Antarctica (e.g., Joughin and Tulaczyk, 2002). The post-breakup velocity is considerably higher, which seems reasonable given that removal of ice shelf buttressing triggers acceleration of grounded ice (De Angelis and Skvarca, 2003).

We compare ice velocities estimated from sediment flux to the expected balance velocity of the paleo-BIS at the time of GZW formation. The balance velocity refers to the ice stream speed at the grounding zone that makes the ice volume discharge equal to the ice volume accumulation. To make this comparison, we take the average accumulation rate for the modern BIS from Joughin and Tulaczyk (2002, their table 1) (136 kg a^{-1} m^{-2}). Constraints from ice cores indicate that the accumulation rate in West Antarctica was comparable to the modern one at the time of Whales Deep Basin GZW deposition (e.g., Buizert et al., 2015, their figure 3b). Other studies have also shown that the paleo–ice accumulation rates in this region were comparable to today's (Waddington et al., 2005). When applied over the entire drainage area (Table 1), this accumulation rate yields a balance mass flux of 32 Gt a^{-1} (Table 2). To convert this into ice volume flux, we estimate average ice column density based on measured pressure in Subglacial Lake Whillans of 7019 kPa and ice thickness of 802 ± 10 m (Tulaczyk et al., 2014). After accounting for acceleration due to gravity, this yields a column-averaged density of 890 ± 10 kg m^{-3}. Dividing the mass flux by the ice column density yields the ice volume flux of $Q = 35.6 \pm 5$ km^3 a^{-1} (Table 2), which can be converted to the balance ice velocity at the grounding line, U_b:

$$U_b = Q/(WH), \quad (3)$$

where W, as before, is the width of the ice stream at the grounding line, while H is the average ice thickness at the grounding line. By inference from the modern bathymetry of the paleo-BIS GZW, H would have been ~550 m for ice to go afloat at the crest of the wedge. Global sea level was 60–80 m lower at the time of GZW deposition, but the bathymetry was also glacioisostatically depressed following the loading by the expanded West Antarctic Ice Sheet during the LGM. Moreover, GZW aggradation itself would have changed the local water depth at the grounding line throughout the period of its deposition (Figs. 1D and 1E). Hence, we assume that H was 600 ± 100 m over the period of GZW formation, yielding a balance ice velocity of 580 ± 100 m a^{-1} from Equation 3 (Table 2).

Figure 2A shows the ratio of ice velocity calculated from sediment flux (Equation 2) to the balance velocity. The baseline case of sediment flux rate averaged over the entire Whales Deep Basin GZW duration, 1.7 ± 0.77 × 10^8 m^3 a^{-1} (Table 1), is shown in black contour lines and black labels. Assuming basal sediment transport parameters ($f = 1$, $h = 3.4 \pm 0.6$ m; Christoffersen et al., 2010), the GZW may have been constructed with ice velocities at the grounding line being comparable to the balance velocity. Observations from seismic profiles indicate that the sediment accumulated before the ice-shelf breakup represents a relatively small fraction

[1]GSA Data Repository item 2020082, supplemental information and previous data, is available online at http://www.geosociety.org/datarepository/2020/, or on request from editing@geosociety.org.

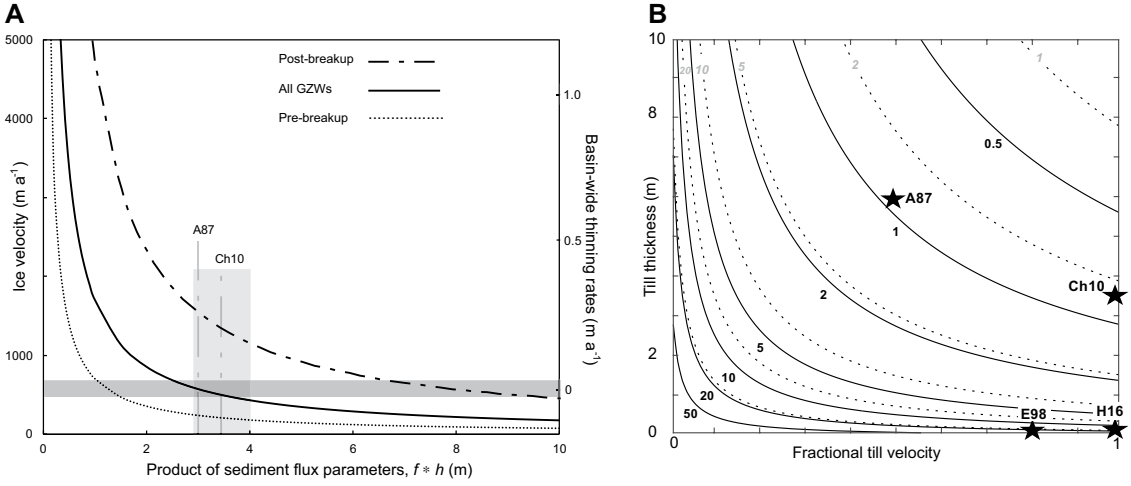

Figure 2. (A) Plot of ice velocity calculated from sediment fluxes as a function of the product of sediment flux parameters *f* (fraction of ice-stream flow velocity) and *h* (effective sediment thickness) (see Equation 2 in text) for the three sediment flux rates corresponding to the entire period of Whales Deep Basin grounding-zone wedge (GZW) deposition (solid black line), pre–ice-shelf breakup phase (dotted black line), and post–breakup phase (dashed black line). Horizontal gray rectangle designates the range of estimated balance ice velocities for the paleo–Bindschadler Ice Stream drainage basin (580 ± 100 m a^{-1}). Vertical dash-dot gray line labeled Ch10 gives our baseline scenario (3.4 m, from Christoffersen et al. [2010]), and the similar line labeled A87 shows $f \times h = 3$ m (Alley et al., 1987) for comparison. (B) Calculated paleo-ice-stream velocity as a function of the two sediment flux parameters, *h* and *f*. Velocity has been non-dimensionalized by dividing it by the estimated balance velocity of the paleo–ice stream, 580 m a^{-1}. Solid contour lines represent velocities calculated using the average sediment flux rate, *q* (1.7 × 10^8 m^3 a^{-1}) over the entire period of GZW deposition (Table 1). Dotted contour lines correspond to ice velocities calculated from the post–ice-shelf breakup sediment flux rate (Table 1). Four labeled stars designate four studies that provide the basis for quantifying the two sediment flux parameters, *h* and *f*. In this manuscript, we mostly use parameter values from Alley et al. (1987) (labeled A87) and Christoffersen et al. (2010) (labeled Ch10) (e.g., see Fig. 1) because using other two options, Engelhardt and Kamb (1998) (labeled E98) and Hodson et al. (2016) (labeled H16) would result in implausibly high paleo–ice stream velocities.

TABLE 2. INFERRED CHARACTERISTICS OF THE PALEO–BINDSCHADLER ICE STREAM, WEST ANTARCTICA

Average ice accumulation rate, modern BIS* (kg a^{-1} m^{-2})	Paleo-BIS drainage area (m^2)	Balance mass flux† (10^{12} kg a^{-1})	Ice column density# (kg m^{-3})	Accumulated ice volume flux§ (km^3 a^{-1})	Balanced ice stream velocity** (m a^{-1})	Discharged ice volume (km^3 a^{-1})	Paleo-BIS mass balance†† (km^3 a^{-1})	Paleo-BIS mass balance†† (Gt a^{-1})
136	2.33×10^{11}	31.7	890 ± 10	35.6 ± 5	580 ± 100	35.6 ± 5	0	0
		Pre-ISBU flow		35.6 ± 5	200 ± 90	12 ± 5	23.6 ± 7	21.0 ± 6
		Post-ISBU flow		35.6 ± 5	1350 ± 580	81 ± 34	–45.4 ± 34	–40.4 ± 30

Note: BIS—Bindschadler Ice Stream.
*From Joughin and Tulaczyk (2002).
†i.e., the product of the first two columns; note that 31.7×10^{12} kg a^{-1} = 31.7 Gt a^{-1}.
#See text for explanation.
§Calculated by dividing balance mass flux by ice column density.
**Row 1 value is from text Equation 3, with $W = 10^5$ m and $H = 600$ m. The lower two rows (shaded in gray) show the ice stream velocities that we estimated from sediment flux (see text for explanation) for the times pre– and post–ice-shelf breakup (ISBU—ice-shelf breakup); G) Average discharged ice volume for the entire grounding is shown in row 1.
(Note: Rows in gray show the discharge estimated from the velocities in this column.)
††i.e., 35.6 km^3 a^{-1} minus the accumulated ice volume flux value. The paleo-BIS mass balance after ISBU was comparable to that currently being discharged from the Pine Island and Thwaites Glaciers.

of the total GZW volume (Bart et al., 2017b) (Table 1; Figs. 1C and 1D). Based on individual seismic profiles with well-resolved internal boundaries, we estimate that 70% ± 10% of the GZW volume accumulated in the relatively brief period after the ice-shelf breakup (Table 1). Under our two-phase scenario, the sediment flux rate increased nearly sevenfold after the ice-shelf breakup, and the ice velocity calculated from Equation 2 with parameters from Christoffersen et al. (2010) is double the balance velocity for this period of time.

Importance of Grounding-Zone Sedimentation

The data presented in Table 1 indicate the importance of incorporating sediment erosion and delivery to grounding lines into numerical ice stream and ice sheet modeling, because the data support the contention that rapid GZW growth may help stabilize grounding-zone position (Alley et al., 2007). In the Whales Deep Basin, the overlapping stack of GZWs has a maximum thickness of 140 m (Fig. 1B) (Bart et al., 2017a). The maximum thickness indicates that sediment aggradation occurred at an average rate of ~40 mm a^{-1} over 3200 ± 700 years, during which global sea level rose by ~30 m (Peltier and Fairbanks, 2006). The relatively low melt rates at the grounding zone of modern Siple Coast ice streams (e.g., Begeman et al., 2018) suggest that although an ample supply of basal debris arrives at the grounding zone, it may not be released fast enough to aggrade large GZWs.

A Highly Negative Mass Balance following Paleo-BIS Ice-shelf Breakup Preceded Major Grounding-Zone Retreat

The long-term average paleo-BIS velocity of ~500 ± 120 m a^{-1} for the entire 3200 yr grounding stillstand (Table 1) suggests that the average annual discharge of ice from the paleo-BIS was 30 ± 7 km^3 a^{-1} (calculated using $W = 100$ km and $H = 0.6$ km). That estimate of ice discharge can be compared with the ice accumulation calculated in the previous section (35.6 ± 5 km^3 a^{-1}; Table 2) to investigate ice sheet mass-balance changes prior to and after ice-shelf breakup. Prior to breakup, the paleo-BIS velocity was 200 m a^{-1}. Ice shelf buttressing may have contributed to the slower ice stream velocity and lower ice volume discharge. Despite an estimated positive mass balance of 23.6 ± 7 km^3 a^{-1} prior to ice-shelf breakup (Table 2), the grounding zone did not advance, suggesting that the ice stream system may have intermittently experienced thickening. Conversely, after breakup, the paleo-BIS appears to have accelerated to 1350 ± 580 m a^{-1} (Tables 1 and 2). The faster flow would equate to an annual ice volume discharge of 81 ± 34 km^3 a^{-1} (Table 2). There was no significant change in the average ice accumulation rate pre– and post–ice-shelf breakup (Buizert et al., 2015); hence, this high discharge would have exceeded the estimated average accumulation (35.6 ± 5 km^3 a^{-1}) and produced a mass balance of – 45.4 ± 34 km^3 a^{-1} (Table 2, after breakup), equivalent to a basin-wide thinning rate of 0.2 ± 0.14 m a^{-1}. This magnitude and duration of ice volume loss was sufficient to trigger grounding-zone retreat to a position >200 km upstream of the GZW starting at 11.5 ± 0.3 cal. kyr B.P. (Bart et al., 2018).

This mass balance for the paleo-BIS after ice-shelf breakup (–45.4 ± 34 km^3 a^{-1}) is comparable to the volume losses currently being experienced by Pine Island and Thwaites drainage basins (68 and 39 km^3 a^{-1}, respectively; Rignot et al., 2019). At present, Pine Island and Thwaites Glaciers are both buttressed by relatively small ice shelves. The comparison of those ice volume losses with that of paleo-BIS suggests that if such losses are sustained and/or accelerated by further destabilization of the ice shelf, then the current drainage into the Amundsen Sea sector may experience a drawdown of the type that preceded the major >200 km retreat of the paleo-BIS (McGlannan et al., 2017; Kingslake et al., 2018; Bart et al., 2018). Our analysis suggests that future evolution of grounding-line positions in the Amundsen Sea region will also be affected by the rate of sediment supply to grounding zones. For instance, if Pine Island and Thwaites Glaciers contain relatively little basal debris, or if such debris is not melted out near the grounding zone, then the ice streams may rapidly recede instead of maintain a relatively stationary grounding position for several hundred years after ice shelf loss as was the case for the paleo-BIS.

CONCLUSIONS

Our quantitative analysis of the Whales Deep Basin GZW indicates that its formation over 3200 ± 500 years can be explained by ice flow velocities that were comparable to the estimated balance velocity of the paleo-BIS as long as sediment flux rates in subglacial deforming till and/or basal transport are as high as has been suggested by Alley et al. (1987) and/or Christoffersen et al. (2010). However, because seismic profiles suggest that the majority of the GZW volume, ~70% ± 10%, was deposited in only 800 ± 300 years after the breakup of the fringing ice shelf, we favor a two-phase scenario for the dynamics of the paleo-BIS during GZW deposition. During the ice shelf phase, which lasted for 2400 ± 400 years, the estimated ice stream velocity was well below the balance velocity, 200 ± 90 m a^{-1} versus 580 ± 100 m a^{-1}. We calculate that after ice-shelf breakup, the ice stream accelerated to 1350 ± 580 m a^{-1}, which far exceeds the balance velocity. This imbalance would have caused basin-averaged thinning of 160 ± 65 m, which may have ultimately contributed to the final retreat of the grounding zone from the Whales Deep Basin GZW. This sequence of events bears resemblance to the recent changes experienced by Pine Island and Thwaites Glaciers and substantiates the concern that these two modern ice streams, which together drain about a third of the marine-based West Antarctic Ice Sheet, may experience significant and rapid future retreat. Our work also points to the need to study the past and present rates of grounding-zone deposition for these ice streams as part of the larger scientific effort to evaluate how much and how fast they will contribute to global sea-level rise.

ACKNOWLEDGMENTS

Bart was supported by U.S. National Science Foundation (NSF) research grant 1246357. Tulaczyk was supported by NSF research grant 1739027, which is part of the NSF and Natural Environment Research Council (NERC)–funded International Thwaites Glacier Collaboration. We thank the captain and crew of the R/V *Nathaniel B. Palmer* for their help in acquiring seismic data during expedition NBP1502B. We also thank the members of the NBP1502 shipboard party for assisting our efforts in the field. We thank Poul Christoffersen, Claus-Dieter Hillenbrand, and Rebecca Totten Manzoni for their reviews that greatly improved the manuscript.

REFERENCES CITED

Alley, R.B., Blankenship, D.D., Bentley, C.R., and Rooney, S.T., 1986, Deformation of till beneath ice stream B, West Antarctica: Nature, v. 322, p. 57–59, https://doi.org/10.1038/322057a0.

Alley, R.B., Blankenship, D.D., Rooney, S.T., and Bentley, C.R., 1987, Till beneath ice stream B: 3. Till deformation: Evidence and implications: Journal of Geophysical Research, v. 92, p. 8921–8929, https://doi.org/10.1029/JB092iB09p08921.

Alley, R.B., Anandakrishnan, S., Dupont, T.K., Parizek, B.R., and Pollard, D., 2007, Effects of sedimentation on ice-sheet grounding-line stability: Science, v. 315, p. 1838–1841, https://doi.org/10.1126/science.1138396.

Alley, R.B., Anandakrishnan, S., Christianson, K., Horgan, H.J., Muto, A., Parizek, B.R., Pollard, D., and Walker, R.T., 2015, Oceanic forcing of ice-sheet retreat: West Antarctica and more: Annual Review of Earth and Planetary Sciences, v. 43, p. 207–231, https://doi.org/10.1146/annurev-earth-060614-105344.

Anderson, J.B., 1999, Antarctic Marine Geology: Cambridge, UK, Cambridge University Press, 289 p., https://doi.org/10.1017/CBO9780511759376.

Bart, P.J., Anderson, J.B., and Nitsche, F., 2017a, Post-LGM grounding-line positions of the Bindschadler Paleo Ice Stream in the Ross Sea embayment, Antarctica: Journal of Geophysical Research: Earth Surface, v. 122, p. 1827–1844, https://doi.org/10.1002/2017JF004259.

Bart, P.J., Krogmeier, B.J., Bart, M.P., and Tulaczyk, S., 2017b, The paradox of a long grounding during West Antarctic Ice Sheet retreat in Ross Sea: Scientific Reports, v. 7, 1262, https://doi.org/10.1038/s41598-017-01329-8.

Bart, P.J., DeCesare, M., Rosenheim, B.E., Majewski, W., McGlannan, A., 2018, A centuries-long delay between paleo-ice-shelf collapse and grounding line retreat in the Whales Deep Basin, eastern Ross Sea, Antarctica: Scientific Reports, v. 8, 12392, https://doi.org/10.1038/s41598-018-29911-8.

Begeman, C.B., Tulaczyk, S.M., Marsh, O.J., Mikucki, J.A., Stanton, T.P., Hodson, T.O., Siegfried, M.R., Powell, R.D., Christianson, K., and King, M.A., 2018, Ocean stratification and low melt rates at the Ross Ice Shelf grounding zone: Journal of Geophysical Research: Oceans, v. 123, p. 7438–7452, https://doi.org/10.1029/2018JC013987.

Bingham, R.G., et al., 2017, Diverse landscapes beneath Pine Island Glacier influence ice flow: Nature Communications, v. 8, 1618, https://doi.org/10.1038/s41467-017-01597-y.

Buizert, C., et al., 2015, The WAIS Divide deep ice core WD2014 chronology—Part 1: Methane synchronization (68–31 ka BP) and the gas age–ice age difference: Climate of the Past, v. 11, p. 153–173, https://doi.org/10.5194/cp-11-153-2015.

Christoffersen, P., Tulaczyk, S., and Behar, A., 2010, Basal ice sequences in Antarctic ice stream: Exposure of past hydrologic conditions and a principal mode of sediment transfer: Journal of Geophysical Research, v. 115, F03034, https://doi.org/10.1029/2009JF001430.

Danielson, M., and Bart, P.J., 2019, Topographic control on the post-LGM grounding zone locations of the West Antarctic Ice Sheet in the Whales Deep Basin, Eastern Ross Sea: Marine Geology, v. 407, p. 248–260, https://doi.org/10.1016/j.margeo.2018.11.001.

Davey, F., and Nitsche, F., 2005, Bathymetric grid of the Ross Sea, Antarctica: http://www.marine-geo.org/tools/search/Files.php?data_set_uid=20275.

De Angelis, H., and Skvarca, P., 2003, Glacier surge after ice shelf collapse: Science, v. 299, p. 1560–1562, https://doi.org/10.1126/science.1077987.

Engelhardt, H., and Kamb, B., 1998, Basal sliding of Ice Stream B, West Antarctica: Journal of Glaciology, v. 44, p. 223–230, https://doi.org/10.1017/S0022143000002562.

Hodson, T.O., Powell, R.D., Brachfeld, S.A., Tulaczyk, S., Scherer, R.P., and the WISSARD Science Team, 2016, Physical processes in Subglacial Lake Whillans, West Antarctica: Inferences from sediment cores: Earth and Planetary Science Letters, v. 444, p. 56–63, https://doi.org/10.1016/j.epsl.2016.03.036.

Jakobsson, M., Anderson, J.B., Nitsche, F.O., Gyllencreutz, R., Kirshner, A.E., Kirchner, N., O'Regan, M., Mohammad, R., and Eriksson, B., 2012, Ice sheet retreat dynamics inferred from glacial morphology of the central Pine Island Bay Trough, West Antarctica: Quaternary Science Reviews, v. 38, p. 1–10, https://doi.org/10.1016/j.quascirev.2011.12.017.

Joughin, I., and Tulaczyk, S., 2002, Positive mass balance of Ross ice streams, West Antarctica: Science, v. 295, p. 476–480, https://doi.org/10.1126/science.1066875.

Kingslake, J., Scherer, R.P., Albrecht, T., Coenen, J., Powell, R.D., Reese, R., Stansell, N.D., Tulaczyk, S., Wearing, M.G., and Whitehouse, P.L., 2018, Extensive retreat and re-advance of the West Antarctic Ice Sheet during the Holocene: Nature, v. 558, p. 430–434, https://doi.org/10.1038/s41586-018-0208-x.

Klages, J.P., Kuhn, G., Hillenbrand, C.-D., Graham, A.G.C., Smith, J.A., Larter, R.D., Gohl, K., and Wacker, L., 2014, Retreat of the West Antarctic Ice Sheet from the western Amundsen Sea shelf at a pre- or early LGM stage: Quaternary Science Reviews, v. 91, p. 1–15, https://doi.org/10.1016/j.quascirev.2014.02.017.

McGlannan, A.J., Bart, P.J., Chow, J.M., and DeCesare, M., 2017, On the influence of post-LGM ice shelf loss and grounding zone sedimentation on West Antarctic ice sheet stability: Marine Geology, v. 392, p. 151–169, https://doi.org/10.1016/j.margeo.2017.08.005.

Mosola, A.B., and Anderson, J.B., 2006, Expansion and rapid retreat of the West Antarctic Ice Sheet in eastern Ross Sea: Possible consequence of over-extended ice streams?: Quaternary Science Reviews, v. 25, p. 2177–2196, https://doi.org/10.1016/j.quascirev.2005.12.013.

Ó Cofaigh, C., Pudsey, C.J., Dowdeswell, J.A., and Morris, P., 2002, Evolution of subglacial bedforms along a paleo-ice stream, Antarctic Peninsula continental shelf: Geophysical Research Letters, v. 29, no. 8, https://doi.org/10.1029/2001GL014488.

Pattyn, F., 2018, The paradigm shift in Antarctic ice sheet modeling: Nature Communications, v. 9, 2728, https://doi.org/10.1038/s41467-018-05003-z.

Peltier, W.R., and Fairbanks, R.G., 2006, Global glacial ice volume and Last Glacial Maximum duration from an extended Barbados sea level record: Quaternary Science Reviews, v. 25, p. 3322–3337, https://doi.org/10.1016/j.quascirev.2006.04.010.

Prothro, L.O., Simkins, L.M., Majewski, W., and Anderson, J.B., 2018, Glacial retreat patterns and processes determined from integrated sedimentology and geomorphology records: Marine Geology, v. 395, p. 104–119, https://doi.org/10.1016/j.margeo.2017.09.012.

Rignot, E., Casassa, G., Gogineni, P., Krabill, W., Rivera, A., and Thomas, R., 2004, Accelerated ice discharge from the Antarctic Peninsula following the collapse of Larsen B ice shelf: Geophysical Research Letters, v. 31, L18401, https://doi.org/10.1029/2004GL020697.

Rignot, E., Mouginot, J., Scheuchl, B., van den Broeke, M., van Wessem, M.J., and Morlighem, M., 2019, Four decades of Antarctic Ice Sheet mass balance from 1979–2017: Proceedings of the National Academy of Sciences of the United States of America, v. 116, p. 1095–1103, https://doi.org/10.1073/pnas.1812883116.

Scambos, T., Fricker, H.A., Liu, C.-C., Bohlander, J., Fastook, J., Sargent, A., Masson, R., and Wu, A.-M., 2009, Ice shelf disintegration by plate bending and hydro-fracture: Satellite observations and model results of the 2008 Wilkins ice shelf break-ups: Earth and Planetary Science Letters, v. 280, p. 51–60, https://doi.org/10.1016/j.epsl.2008.12.027.

Tulaczyk, S., Kamb, W.B., and Engelhardt, H.F., 2000, Basal mechanics of Ice Stream B, West Antarctica: 2. Undrained plastic bed model: Journal of Geophysical Research, v. 105, p. 483–494, https://doi.org/10.1029/1999JB900328.

Tulaczyk, S., Mikucki, J.A., Siegfried, M.R., Priscu, J.C., Barcheck, C.G., and Beem, L.H., 2014, WISSARD at Subglacial Lake Whillans, West Antarctic: Scientific operations and initial observations: Annals of Glaciology, v. 55, p. 51–58, https://doi.org/10.3189/2014AoG65A009.

Vieli, A., Payne, A.J., Shepherd, A., and Du, Z., 2007, Causes of pre-collapse changes of the Larsen B ice shelf: Numerical modelling and assimilation of satellite observations: Earth and Planetary Science Letters, v. 259, p. 297–306, https://doi.org/10.1016/j.epsl.2007.04.050.

Waddington, E.D., Conway, H., Steig, E.J., Alley, R.B., Brook, E.J., Taylor, K.C., and White, J.W.C., 2005, Decoding the dipstick: Thickness of Siple Dome, West Antarctica, at the Last Glacial Maximum: Geology, v. 33, p. 281–284, https://doi.org/10.1130/G21165.1.

Printed in USA